Intriguing I_2 Reduction in the Iodide for Chloride Ligand Substitution at a Ru(II) Complex: Role of Mixed Trihalides in the Redox Mechanism

Marta E.G. Mosquera,*,‡ Pilar Gomez-Sal,*,‡ Isabel Diaz,‡ Lina M. Aguirre,‡ A. Ienco,‖ Gabriele Manca,‖ Carlo Mealli.*, ‖

‡ Dpto de Química Orgánica y Química Inorgánica, Universidad de Alcalá, Campus Universitario, E-28871 Alcalá de Henares, Spain.

‖ Consiglio Nazionale delle Ricerce, Istituto di Chimica dei Composti Organometallici (CNR-ICCOM), Via Madonna del Piano 10, 50019 Sesto Fiorentino (FI). Italy.

ABSTRACT.

The compound $[Ru(CN^tBu)_4(Cl)_2]$, **1**, reacts with I_2 yielding the Halogen-Bonded (XB) 1D species $\{[Ru(CN^tBu)_4(I)_2]\cdot I_2\}_n$, $(\mathbf{2\cdot I_2})_n$, whose building block contains I^- in place of Cl^- ligands, even though no suitable redox agent is present in solution. Some isolated solid state intermediates, such as $\{[Ru(CN^tBu)_4(Cl)_2]\cdot 2I_2\}_n$, $(\mathbf{1\cdot 2I_2})_n$ and $\{[Ru(CN^tBu)_4(Cl)(I)]\cdot 3I_2\}_n$, $(\mathbf{3\cdot 3I_2})_n$ indicate the stepwise substitution of the two *trans* halide ligands in **1**, showing that end-on coordinated trihalides play a key role in the process. In particular, the formation of ClI_2^- starts triggering electron transfer, possibly followed by an inverted coordination of the triatomic through the external iodine atom. This allows I-Cl separation, as corroborated by RAMAN spectra. The process through XB intermediates corresponds to reduction of one iodine atom combined with the oxidation of one coordinated chloride ligand to give the corresponding zero-valent atom of I-Cl. This redox process, explored by DFT calculations (B97D/6-31+G(d,p)/SDD(for I and Ru atoms), is apparently counterintuitive with respect to the known

behavior of the corresponding free halogen systems, which favor iodide oxidation by Cl_2. On the other hand, similar energy barriers are found for the metal-assisted process and require a supply of energy to be passed. In this respect, the control of the temperature is fundamental in combination with the favorable crystallizations of the various solid state products. As an important conclusion, trihalogens, as XB adducts, are not static in nature but able to undergo dynamic inner electron transfers consistently with implicit redox chemistry.

INTRODUCTION

Halogen bonding (XB)[1] is a non-covalent interaction between one terminal halogen atom (X) and a base (D). Although known for a long time its importance has been particularly acknowledged in the past 20 years and is now recognized to be relevant in a variety of fields from materials[2] to biological systems.[3] Our groups have previously studied fully halogen-based XB systems from both experimental[4] and theoretical[5] points of view. In our aim for designing new networks based on the XB interactions, we studied the suitability of $[Ru(CN^tBu)_4(Cl)_2]$ (**1**) as XB acceptor. The choice of this metallic fragment in based on the intrinsic interest of Ru(II) compounds due their remarkable activity in areas such as catalysis,[6] biomedicine[7] or photochemistry.[8] In those areas, also the role of XB interactions has been increasingly acknowledged in recent years,[2,3,8c,9] as for example in the XB-induced carbon-carbon bond formation described by Stefan H. Huber,[9b] the importance of the XB in the deiodinase activity reported by Mugesh[9c] or its influence on regeneration of the oxidized dye in DSSCs (dye-sensitized solar cells) studied by Haukka.[8c] In this latter case a fundamental role is played by trihalides, a limiting example of XB where the base is a halide itself and the halogen donor group (Y-X) is the dihalogen unit.

Advancing in the knowledge of how the formation of a XB network would affect $[Ru(CN^tBu)_4(Cl)_2]$ (**1**) properties drove us to study its reaction with I_2. Unexpectedly, the resulting species was a new compound, with iodide in place of the original chloride ligands, $[Ru(CN^tBu)_4(I)_2]$ (**2**). The latter complex is involved in the solid state networks of formula $\{[Ru(CN^tBu)_4(I)_2]\cdot I_2\}_n$ $(\mathbf{2\cdot I_2})_n$ with I_2 linkers between adjacent building blocks. In the lack of any suitable redox agent for the I_2 reduction in solution, the transformation of **1** in **2** seems only justified by an electron transfer between the different halogen species and through the formation of XB adducts. Since the analogous process for the corresponding free halogen system is reversed, the metal center seems to play a key role in this intriguing chemistry. To shed some light on the process, systematic synthetic studies were carried out, which successfully led to the isolation of some key intermediates. On their basis, possible reaction profiles could be proposed also by seeking the corroboration of DFT calculations, carried out with the model chemistry B97D[10]/6-31+G(d,p)/SDD(for I and Ru atoms).[11] This paper illustrates in details the unexpected chemical behavior of the mixed interhalogen system and their counterintuitive chemical reactivity. The particularly important result is that electron transfer (redox) capabilities can be operative in dynamically behaving XB systems.

RESULTS AND DISCUSSION

Halide ligands in transition metal complexes have been frequently seen as halogen acceptors in XB networks.[12] In this context, we investigated the suitability of complexes of the type $[RuL_4(Cl)_2]$ as building blocks for the generation of supramolecular networks. In particular, we focused on the known species $[Ru(CN^tBu)_4(Cl)_2]$ (**1**),[13] whose structure was not reported before. This is now confirmed to be an octahedral Ru(II) complex with two *trans* chloride ligands and four *equatorial* isocyanide ones, all with standard geometric parameters as reported in Table 1.

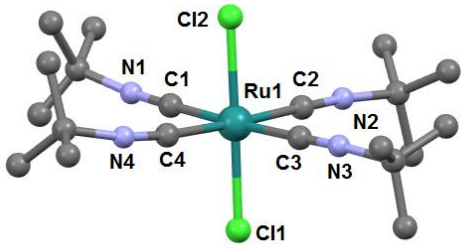

Figure 1. The precursor complex [Ru(CN^{t}Bu)$_4$ (Cl)$_2$] (**1**).

Table 1. Selected Bond lengths [Å] for compound **1,** **(1·2I$_2$)$_n$** , **(2·I$_2$)$_n$** and **(3·3I$_2$)$_n$.**

1[a]		**(1·2I$_2$)$_n$**[b]		**(2·I$_2$)$_n$**[c]		**(3·3I$_2$)$_n$**[d]	
				Bond lengths			
Ru(1)-Cl(2)	2.4049(19)	Ru(1)-C(1)	2.004(14)	Ru(1)-C(11)	1.996(5)	Ru(1)-C(2)	2.01(3)
Ru(1)-Cl(1)	2.4209(18)	Ru(1)-Cl(1)	2.448(4)	Ru(1)-C(1)	2.003(5)	Ru(1)-C(1)	2.08(3)
Ru(1)-C(range)	1.987(7) – 1.993(7)	Cl(1)···I(2)	3.110(2)	Ru(1)-I(1)	2.7420(8)	Ru(1)-Cl(1)	2.485(9)
		I(2)-I(2)#4	2.724(2)	I(2)-I(2)#2	2.7655(8)	Ru(1)-I(1)	2.633(5)
Ru(2)-Cl(3)	2.405(2)	C(1)-N(1)	1.12(2)	I(1)···I(2))#1	3.3153(7)	I(1)···I(7)	3.140(4)
Ru(2)-Cl(4)	2.4237(18)	Cl(1)···I(2)#2	3.110(2)			I(2)-I(7)	2.749(4)
Ru(2)-C(range)	1.984(7) – 1.993(7)					I(3)-I(4)	2.734(5)
						I(5)-I(6)	2.704(5)
						I(1)···I(4)	3.309(5)
						Cl1(1)···I(3)	3.056(5)
						Cl1(1)···I(6)#2	2.894(8)

[a] Two independent molecules are observed in the unit cell
[b] Symmetry transformations used to generate equivalent atoms:#1 -x,-y,-z #2 x,y,-z #3 -x,-y,z #4 -x,-y+1,-z
[c] Symmetry transformations used to generate equivalent atoms: #1 -x+1,y,-z+3/2 #2 -x+2,y,-z+3/2
[d] Symmetry transformations used to generate equivalent atoms: #1 x,-y+1/2,z; #2 x+1/2,y,z+3/2

Treatment of complex **1** with I_2 originates the particularly rich chemistry illustrated in this paper. As such, when the reaction is performed at room temperature in CH_2Cl_2 solution and under argon atmosphere, brown crystals could be isolated. A X-ray analysis of this product showed, as an unexpected result, the formation of the corresponding iodide derivative [Ru(CN^{t}Bu)$_4$(I)$_2$] (**2**), as a building block of a solid state compound. Thus, in the absence of any suitable redox agent in solution, the surprising I_2 reduction possibly occurs as suggested in Scheme 1, where the co-product is the interhalogen diatomic I-Cl. The same process also occurs in methanol solution in a shorter reaction time.

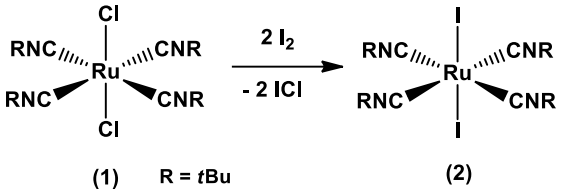

Scheme 1. Reaction of the formation of **2.**

From the crystalline packing, a 1D species is observed where the molecules of **2** are associated as ribbons by XB interactions with diiodine molecules in agreement with the formula $(\mathbf{2}\cdot\mathbf{I_2})_n$ (Figure 2 and Table 1). The pattern of $(\mathbf{2}\cdot\mathbf{I_2})_n$ has been previously observed in other similar 1D compounds, involving different halide or thiocyanate apical ligands.[14]

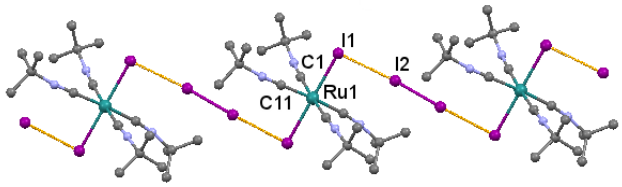

Figure 2. The 1D ribbon $\{[Ru(CN^tBu)_4I_2]\cdot I_2\}_n$, $(\mathbf{2}\cdot\mathbf{I_2})_n$.

From another point of view, $(\mathbf{2}\cdot\mathbf{I_2})_n$ can be seen as formed by linear I_4^{2-} dianions,[15] which interconnect bare $\{Ru(CNR)_4\}^{2+}$ planar fragments. Some of us have previously analyzed the electronic nature of discrete I_4^{2-} species found in several crystal structures and showed that the lateral I-I linkages are much weaker than the central one. The effect was clearly attributable to the external counterions, which favor a higher electron density localization at the terminal atoms.[5] In the case of $(\mathbf{2}\cdot\mathbf{I_2})_n$, the large and localized 2+ charge of the metal ion evidently reinforces the lateral interactions, which are amongst the shortest ever found (3.3153(7) Å). [16]

As a variance with the present chemistry centered on the I_2 reduction, the iodide for chloride ligand substitution most easily occurs when I^- anions are directly added to the solution or a suitable reducing agent of I_2 is employed. Here, the problem arises of the puzzling *in-situ* generation of iodides from the pure solid I_2 reactant. A photochemical mechanism or the possible

metal participation through the Ru(II)→Ru(III) oxidation was excluded because the reaction did not change by operating in the dark or under daylight. As well, the NMR spectroscopy highlights the persistent diamagnetism of the system. It has been reported for related species of type **1**, that the attainment of Ru(III) derivative of $[Ru(CNPh)_4Cl_2]$ occurs at the electrochemical potential of +1.55 V (*vs*. SCE) or requires a strong oxidant such as Ce(IV) salt (the Ce(IV)/Ce(III) redox potential is +1.72 V).[17] It is therefore highly improbable that the I_2 alone can lead to the oxidation of Ru(II) to Ru(III) in the case of **1**, given that the I_2/I^- redox potential is only 0.53 V (*vs*. SCE). In this respect, *ad-hoc* DFT calculations indicate a high energy cost (+36 kcal mol^{-1}) for the I_2 reduction associated to the formation of a Ru(III) complex (see Scheme S1). Moreover, another potential oxidant such as oxygen is excluded as the reaction takes place under argon atmosphere.

Since also the isocyanides molecules remain unaltered in the process, only the original chloride ligands in **1** can act as the reducing agent. Such an hypothesis appears however counterintuitive in view of the available experimental redox potentials of the various $X_2/2X^-$ redox couples for free halogens.[18] From these data, it clearly emerges that the reverse I^- oxidation by Cl_2 is most probable, since the process of Eq. 1 (Scheme 2) is -37.9 kcal mol^{-1} exergonic.

$$Cl_{2(g)} + 2I^-_{(sol)} \rightarrow I_2 + 2Cl^-_{(sol)} \quad \text{Eq 1}$$

Scheme 2. The spontaneous iodide/chloride interconversion.

By assuming that the formation of the single unit **2** or the compound $(\mathbf{2}\cdot\mathbf{I_2})_n$ is not a first order process, attempts were made to detect possible intermediates. Thus, a rapid crystallization procedure, following the I_2 addition to **1**, afforded the isolation of dark-red crystals, which correspond to $\{[Ru(CN^tBu)_4(Cl)_2]\cdot 2I_2\}_n$ $(\mathbf{1}\cdot\mathbf{2I_2})_n$ according to X-ray diffraction analysis. As shown in Figure 3, still intact building blocks of **1** are connected by I_2 molecules as linkers, to give a 2D network of the honey-comb type (**hcb**[19]). This is first direct evidence that XB interactions play an active role in the reactivity. In the arrangement, each *trans*-axial chloride

ligand uses both its orthogonal p_π lone pairs to attack distinct I_2 molecules and form ClI_2Cl^{2-} linkers. Such a moiety has been previously observed only in a Fe(III) binuclear system,[20] whereas in $(\mathbf{1}\cdot\mathbf{2I_2})_n$ each chloride ligand forms a local V-shaped ClI_4^- anion as a part of a large 16-membered ring. Both features are unprecedented, but it must be mentioned that isolated I_5^- species are known.[21]

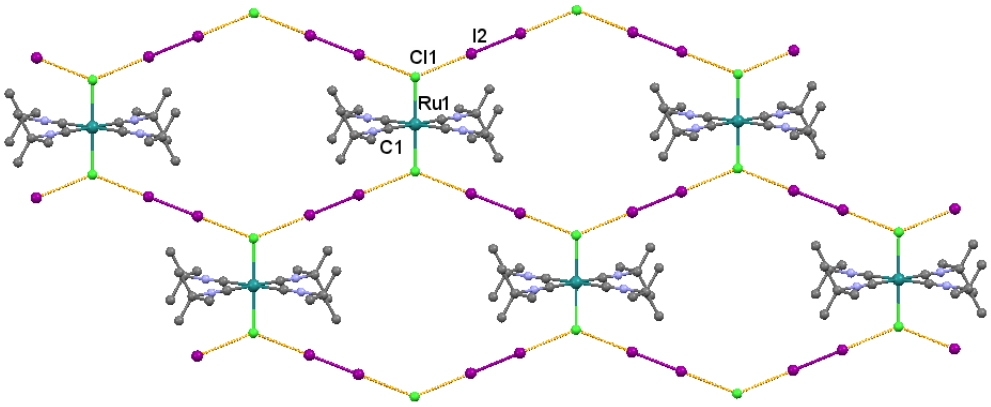

Figure 3. 2D network for $\{[Ru(CN^tBu)_4(Cl)_2]\cdot 2I_2\}_n$ $(\mathbf{1}\cdot\mathbf{2I_2})_n$ (Cl···I 3.110(2) Å, I···Cl···I 135.51(5)°).

If the crystallization leading to $(\mathbf{1}\cdot\mathbf{2I_2})_\mathbf{n}$ is inhibited and the reaction is allowed to evolve for a longer period of time, or heated at 40°C, the new isolated crystals show another solid state structure, still supported by an important XB network. Here, the metal building block describe as $[Ru(CN^tBu)_4(Cl)(I)]$, (**3**), apparently derived from the substitution of one Cl^- ligand for I^- in **1** (Scheme 3).

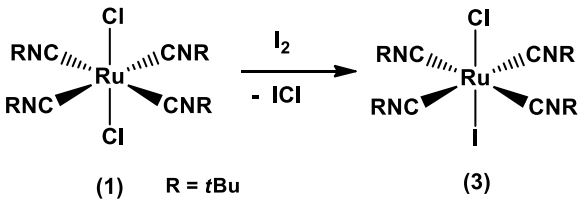

Scheme 3. Generation of the building block **3.**

The crystal packing of Figure 4 shows that different halide ligands of **3** interact with distinct I_2 molecules to form end-on coordinated I_3^- and ClI_2^- trihalides,[22] with the corresponding I-I distances being 2.749(4) and 2.704(5) Å, respectively, hence a more appropriate formulation of the building block is $\{Ru(CN^tBu)_4(I_3)(ClI_2)\}$. These metal units are pairwise interconnected by I_2 molecules generating the 1D solid state system of formula $\{[Ru(CN^tBu)_4(Cl)(I)]\cdot 3I_2\}_n$ (**3·3I₂**)$_n$.

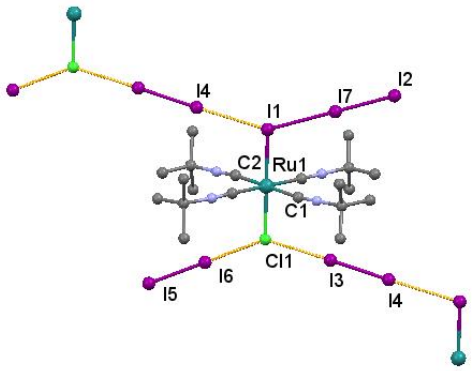

Figure 4. Structure of the intermediate $\{[Ru(CN^tBu)_4(Cl)(I)]\cdot 3I_2\}_n$ (**3·3I₂**)$_n$. Relevant bonds: (Cl(1)···I(6) 2.894(8) Å, Cl(1)···I(3) 3.056(5) Å, I(1)···I(4) 3.309(5) Å, I(1)···I(7) 3.140(4) Å).

As reported in Table 1, the terminal I-I linkage in both the I_3^- and ClI_2^- apical ligands is barely elongated with respect to free I_2, whereas the collinear vectors involving the coordinated halide ligand are clearly larger, possibly due to the close 2+ metal charge.[5] The larger Cl-I and I-I distances in the terminal trihalides are however shorter than the corresponding side vectors of the ClI_3^{2-} linker (2.894(8) *vs*. 3.056(5) Å and 3.140(4) *vs*. 3.309(5) Å, respectively). These features seem to mirror the different distributions of charges and electron density at the various components of the overall XB system. Of particular interest is the end-on coordinated ClI_2^- ligand, which is the best candidate to participate in the redox/substitution processes associated to either the $[Ru(CN^tBu)_4(Cl)_2]$ (**1**) → $[Ru(CN^tBu)_4(Cl)(I)]$ (**3**) or the $[Ru(CN^tBu)_4(Cl)(I)]$ (**3**) → $[Ru(CN^tBu)_4(I)_2]$ (**2**) transformations. In particular, we focus on the first **1→3** path, for which a

possible evolution is suggested in Scheme 4. This implies at some point the heterolytic cleavage of one Ru-Cl coordination bond.

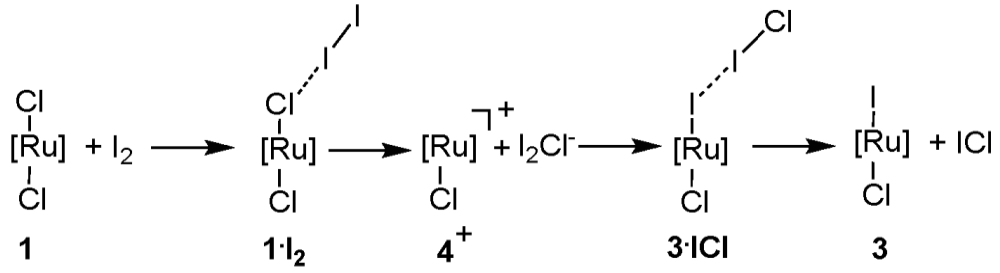

Scheme 4. Possible mechanism for Cl^-/I^- ligand substitution in **1** upon I_2 addition and ICl liberation. [Ru] = $\{Ru(CN^tBu)_4\}^{2+}$.

As shown in Scheme 4, the process may start with the initial formation of one coordinated ClI_2^- trihalide (initial **1·I₂** adduct), followed by the whole ClI_2^- separation. The residual $16e^-$ fragment $\{Ru(CN^tBu)_4(Cl)\}^+$, $\mathbf{4}^+$, is then better stabilized by the same trihalide when coordinating *via* the terminal I atom which is a better donor to give **3·ICl**. It should be pointed out that the formation of unsaturated $\{RuL_5\}^{n+}$ fragments has been previously reported with different ligands.[23] The subsequent I-Cl separation provides **3**, which in presence of I_2 can promptly transform into the discrete complex **3·I₂** and eventually the solid state product $(\mathbf{3\cdot 3I_2})_n$, whose low solubility should favor the crystallization process. If compound **3** remains in solution, another iodide may replace the still present chloride ligand, affording the building block $[Ru(CN^tBu)_4(I)_2]\cdot(\mathbf{2})$ and finally the solid state product $(\mathbf{2\cdot I_2})_n$.

A key aspect in the mechanism of Scheme 3 is that the formation of the iodide ligand implies I_2 reduction and chloride oxidation, as it is implicit in the formal zero-valent halogen atoms of the I-Cl diatomic. In order to detect the formation of I-Cl, the evolution of the reaction in solution was monitored by Raman spectroscopy.[24] The reaction was checked every ten minutes and after

20 minutes the presence of a band at 212 cm^{-1} became apparent. This band can be assigned to the I-Cl generated since it matches the spectra of commercial I-Cl in CH_2Cl_2 (see SI).

The reaction was also monitored by proton NMR spectroscopy. The dichloro complex **1** features a peak at 1.58 ppm, which shifts to 1.62 ppm after the I_2 addition. The result is consistent with the formation of the Cl-Ru-Cl···I_2 adduct, **1·I₂**. Then, two peaks at 1.62 and 1.61 ppm are observed, probably due to compound **3** that starts to be generated. An equilibrium is likely established, since the intensities of the peaks vary over days, depending on the temperature and also on the side crystallization of some components such as **3·3I₂**. It must be underlined that the formation of various crystalline materials implies an important role of the solubility factor in these reactions, with the network for **3** being less soluble than the one based on **1**. To gain further insights into how the reaction between **1** and I_2 proceeds in solution, a study of the aggregation process was performed at various concentrations and reaction times by monitoring the diffusion coefficient D (see SI). In the studied conditions, a clear decrease of the D value was observed after only five minutes and it can be attributed to XB intermolecular interactions between **1** and I_2 (Table S1). Then, D fluctuates in the following days, suggesting that its increase/decrease is due to a sequence of aggregations and dissociations, similar to the behavior of polyhalides in solution. These spectroscopic findings are in agreement with the evolution of **1** to **3** in solution *via* the formation of halogen bonded species.

Theoretical aspect of the electron transfer at the trihalides XB adducts. The proposed mechanism of Scheme 3 was also studied by the DFT methods with the results illustrated below. First however, we briefly address how electron flow may occur through the atoms of the XB adducts, which as trihalides seem to be key intermediates or products of the present chemistry. Indeed, upon the addition of a halide to a dihalogen molecule, evident electron transfer occurs between the two lateral atoms with the central one being unaffected. The latter picture itself

implies a covalent character of XB besides the purely electrostatic one. The point has been similarly underlined by other authors also for Hydrogen Bonding (HB),[25,26] given that the external base D transfers electron density in the Y-H σ* level. On the other hand, the lack of a p axial function at the H atom determines some minor difference with respect to XB. Instead, the classic picture of halogen bonding[1] is mainly focused on static interactions of the electrostatic and polarization type, while the critical charge transfer is much less emphasized, although originally stressed by Mulliken.[27] By referring to the symmetric I_3^- as one of the strongest XB adducts of this type, a net $0.5e^-$ transfer occurs from the entering iodide into the opposite end of I_2, while the central I atom stays zero-charged all the way.[5] The addition is exergonic by -13.3 kcal mol^{-1} hence a new scission can be induced by supplying the equivalent amount of energy to the system. In this case, it may be one fully reduced atom of I_2 to depart in place of the originally entered iodide, implying that an actual redox reaction occurs through the XB adduct at an overall null energy balance. As mentioned, this requires a dynamic control by external factors such as for instance the temperature. Similarly, also the atoms of other interhalogen systems may switch their initial oxidation states and, in principle it cannot be totally excluded that the counterintuitive I_2 reduction by chloride may occur through a controlled electron flow at the XB adduct ClI_2^-. As further discussed below, the sequential association/dissociation of the trihalide has also not negligible entropy components.

The σ electron density in trihalides is largely delocalized, as already underlined by us[5] and other authors.[28] The implicit covalency of the XB systems is also hypervalency[29] because, at variance with the classic Rundle-Pimentel description,[30] the populated s orbital of the central atom plays a critical role consistently with our previously proposed "$6e^-$/4orbitals" model.[31] This offers an easy interpretation for the loss of the $D_{\infty h}$ symmetry detected in several crystal structures of homoleptic trihalides, such as I_3^-.[32] With the help of Hirshfeld surfaces,[33] it was found that this depends on the unbalanced distribution of the external positive counterions and the effect was

mimicked by *ad-hoc* DFT calculations.[5] As a consequence, the delocalized σ electron density accumulates at the lateral I atom most affected by cations, almost as if it was an halogen of higher electronegativity (*e.g.,* I_2Cl^- *vs.* I_3^-). The important orbital implications are highlighted by the HOMO of the system in Scheme 5, which upon the symmetry descent starts exhibiting an otherwise forbidden s/p mixing at the central atom.

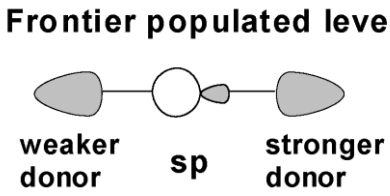

Scheme 5. Effect of the sp rehybridization at the centre of a trihalide due to the electronegativity perturbation at a lateral atom.

The more expanded lobe of the sp hybrid is antibonding toward the electron richer or more electronegative terminal atom (weaker σ donor), hence the distance elongates. Conversely, the collinear linkage to the more powerful lateral σ donor is strengthened due to the bonding between the lone pair and the mixed-in central p orbital.[31] The picture can be generalized for any asymmetric XB system, where the weaker is one lateral donor the easier is its separation. For instance, in the classical species of the type R-I···I^- the aryl/alkyl R group is the strongest donor, hence the lateral iodide interacts only weakly. By increasing the strength of R with electron-donating substituents, the C-I and I-I linkages approach the limiting 1 and 0 bond orders, respectively. Experimentally, a XB adduct survives with fluorinated R groups, as highlighted by some X-ray structures,[34] otherwise any residual I···I interaction tends to disappear in the solid state and more likely in solution. In this respect, a known strategy to form carbo-iodo compounds is to combine I_2 with the carboanion of the R^-Li^+ species.[35] This corresponds to an actual redox reaction, proceeding though a XB intermediate. The border for XB dissociation is rather subtle

and, as mentioned, depends on the substituents at the carboanion. DFT calculations indicate that, while the system $F_3C\text{-}I^{\cdots}I^-$ system is still somewhat exergonic, the $H_3C\text{-}I^{\cdots}I^-$ is already endergonic by +3 kcal mol^{-1}, which is still found as a minimum only thanks to a favorable entropy component. Therefore, entropy has a relevant role on the maintaining or cleaving of the XB adduct and this is subject to a variety of factors, including temperature, abrupt concentration changes of the involved chemical components and more.

The previous considerations on the ruling of the XB interactions are useful in comparing the behavior of free and metal coordinated trihalides. By returning to the textbook case of the reduction of Cl_2 by iodide (Eq. 1 in Scheme 2), the large exergonic balance of -37.9 kcal mol^{-1} leaves little doubt on its evolution. On the other hand, the process must likely proceed through different trihalide intermediates, as indicated in the Eqs. 2 and 3 of Scheme 6. From the calculations, it is found that not all the steps are exergonic for entropy reasons. Indeed, the absolute $|T\Delta S|$ value at any association/dissociation step is as large as ~ 10 kcal mol^{-1} and overwhelms in some case the enthalpy component, with some implication for the reverting of the process. The data in Scheme 6 are also useful to monitor the electron flowing at each step also in view of the changes in the interatomic distances and atomic charges.

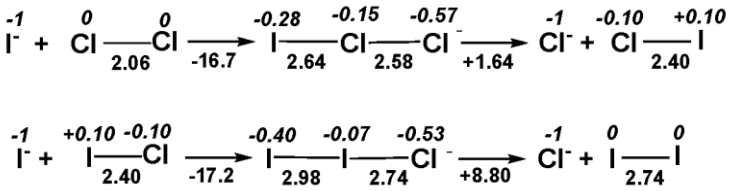

Scheme 6. Variations of geometries, charges and energies in the proposed sequential association/dissociation steps in dichloromethane solution of the cumulative Eq. 1.

In short, the first nucleophilic attack of I^- into Cl_2 (beginning of Eq. 2) is largely exergonic (-16.7 kcal mol^{-1}) and accompanied by the shift of $0.57e^-$ from the entering iodide into the remote

chlorine atom. This seems to foreshadow the subsequent chloride separation from ICl_2^-, the process being only slightly hindered (+1.64 kcal mol^{-1}). On the other hand, such a small loss of energy is promptly compensated by the attack of a second iodide into the residual I-Cl diatomic, since the I_2Cl^- is as exergonic as -17.2 kcal mol^{-1} (first step of Eq. 3). Also, in this case the remote Cl atom accumulates as many as $0.5e^-$, while the central iodine atom has the barely negative charge of -0.07, which is inconsistent with the rather idea that in this type of reactions it would be the central atom to transfer as a cation between lateral anions.[36] In any case, the chloride departure from I_2Cl^- is more difficult than that from ICl_2^- (+8.80 *vs*. +1.64 kcal mol^{-1}), but again the process is feasible if another iodide interacts with I_2 to give I_3^-. This helps to shift the equilibrium and complete the Cl_2 reduction (Eq. 1).

The clearly disfavored I_2 reduction and Cl^- oxidation for free halogen systems does not a-priori exclude that the process is easier over a Ru(II) metal center. Moreover, in our experimental chemistry (Scheme 1), the Cl^- oxidation is limited to I-Cl rather than proceeding all the way to Cl_2, hence its occurrence is more probable. Therefore, the proposed mechanism of Scheme 4 was computationally analyzed by constructing in the CH_2Cl_2 solvent the energy profile of Scheme 7. We are aware that, the trends may be significantly affected by extra-stabilization energies in the generation of solid state compounds, but unfortunately our computational tools were inadequate to tackle crystallization events.

The pathway starts with the I_2 addition to one Cl^- ligand of the model $[Ru]Cl_2$, **1m**, where [Ru] is the fragment $[Ru(CNR)_4]$ with $R=CH_3$ substituents in place of the experimental ^{t}Bu ones. In **1m**, each chloride ligand is already donating $0.60e^-$ to the metal; hence it has limited nucleophilic power toward I_2. Indeed, the formation of ClI_2^- as a ligand is four times less exergonic than that of the corresponding free trihalide (reverse right step of Eq. 3). This is corroborated by the definitely larger Cl-I linkage in the adduct **1m·I₂** *vs* ClI_2^- (2.91 Å *vs.* 2.74 Å) because only $0.3e^-$

are transferred from the Cl^- ligand into the I_2 terminal iodine atom. This also implies a reduced possibility of one iodide dissociation from **1m·I₂**,(Fig.S6) as confirmed by the higher energy cost of such a process with respect to the case of free ClI_2^- (+29.2 *vs.* +17.2 kcal mol^{-1}). The former value was estimated from the successful optimization of the metal complex $\{[Ru]Cl(ClI)\}^+$, **4m·ICl** (Fig. S7), which features the Cl-I diatomic as a ligand. This is a questionable species because, any dihalogen molecule is mainly considered acidic with an almost insignificant $2e^-$ donor capability toward a good σ-acceptor metal atom, such as that of the unsaturated fragment $\mathbf{4m}^+$ (Fig. S8). In actuality, two cases of I_2 coordination are known to occur at the apex of a d^8 square-planar Pt(II) complex,[37] suggesting that bonding is ensured by the filled z^2 metal orbital, as remarked by other authors.[38]

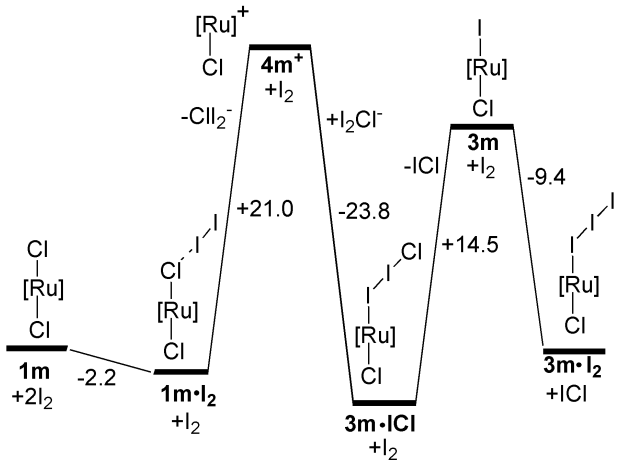

Scheme 7. Energy profile for the I^- for Cl^- ligand upon the reaction of complex **1m** with I_2 reduction ([Ru] = $\{Ru(CNMe)_4\}^{2+}$).

A more concrete evolution of **1m·I₂** is the release of the whole ClI_2^- ligand, although the unsaturated $\mathbf{4m}^+$ species causes a destabilization of +21.0 kcal mol^{-1}, which is also the higher barrier along the reported profile. In any case, the system promptly overcomes the lost energy through the new coordination of the same trihalide via the terminal iodine atom, which is a better donor. In fact, the species **3m·ICl** (Fig. S9) has stabilization energy of -23.8 kcal mol^{-1}. An

advantage of such a reversion is that the I-Cl diatomic may eventually separate at the cost of +14.5 kcal mol^{-1}, which is less penalizing than the analogous dissociation from the free trihalide ClI_2^- (+17.2 kcal mol^{-1}). The difference is already justified by the strong Ru-I linkage in **3m**, but further stabilization may be attained with the presence of additional I_2 molecules in solution. One of them leads to **3m·I₂**, which has an additional energy gain of -9.4 kcal mol^{-1} and is consistent with the terminal I_3^- ligand in the solid state product $(\mathbf{3 \cdot 3I_2})_n$.

As mentioned, the reactivity appears affected by the temperature, since the formation of $(\mathbf{3 \cdot 3I_2})_n$ is definitely faster at 40ºC with respect to RT. On the other hand, the highest barrier in Scheme 7 is +21.0 kcal mol^{-1}, a value which is not prohibitive for a thermodynamically governed process. Similar barriers are also observed for the corresponding free halogen system (Scheme 6), but consider that over the metal the chloride oxidation to I-Cl is more immediate than that to Cl_2. Also, while the metal center is excluded from any redox engagement, it seems to have an anchoring role, which may favor the evolution of the XB trihalide. As well, the kinetic factor seems important for the reactivity, also in view of the significantly large entropy component associated to the association/dissociation of any XB species. This aspect could be properly highlighted by mimicking the complete reaction pathways, but unfortunately our computational tools are inadequate to provide satisfactory quantitative answers to the complex formation/crystallization of the observed solid state products.

Finally the experiments indicate that the counterintuitive redox reactivity is even faster by using MeOH in place of CH_2Cl_2 as a solvent. The computed energy profile is rather similar to that of Scheme 7 (Scheme S2), but the highest barrier for the ClI_2^- dissociation from $\mathbf{4m}^+$ is about 25% lower (+15.6 *vs.* +21.1 kcal mol^{-1}). Additionally, CH_3OH can act as a ligand through its oxygen atom to give the complex $\mathbf{4m^{+} \cdot CH_3OH}$ (Fig. S10). The energy balance for the methanol coordination/de-coordination is only 8.4 kcal mol^{-1} suggesting that the complex in question may

act as a resting state of the metastable yet reactive **4m**$^{+}$ species, which in this manner does not remain unsaturated over long periods of time. Therefore, these results help to clarify the better efficiency of the process in methanol.

CONCLUSIONS

This paper has raised the intriguing substitution of two *trans* chloride ligands of the Ru(II) complex [Ru(CN^{t}Bu)$_4$(Cl)$_2$] (**1**) by iodides, which can only de derived from the reduction of the I_2 reactant. In fact, no suitable reducing agent was present and also the possibly associated Ru(II)→Ru(III) oxidation could be excluded by both the experimental and computational data. The experiments indicated a stepwise process, as suggested by characterized solid state intermediates, such as (**1**·**2I$_2$**)$_n$, and (**3**·**3I$_2$**)$_n$. From the nature of these isolated intermediates, it emerges that an important role for the reactivity is played by the various XB adducts. The presence of these interactions also in solution is corroborated by slight changes in the chemical shifts and also by the diffusion studies. In the proposed mechanism after the first I_2 addition to one chloride ligand of **1**, the trihalide ClI_2^- may separate from the cationic metal fragment {Ru(CN^{t}Bu)$_4$(Cl)}$^{+}$ and it may be coordinated again via its terminal I atom. In this case, the I-Cl dihalogen lays terminal and has the possibility of separating, which is confirmed by Raman spectroscopy. This process implies a redox reaction, given that I-Cl consists of two formally zero-valent halogen atoms, which originate from the combined Cl^- oxidation and I_2 reduction. In this process, the electron flow, which has been indicated by our theoretical modeling to accompany the formation of any XB adduct, must play a fundamental role. DFT calculations and their electronic underpinnings support the mechanism. Barriers are present along the pathway, however there are never excessively high and are likely passed upon an increase of the temperature. Also, significantly large entropy components accompany the

association/dissociation of the various trihalogen species involved in actual electron transfer processes.

EXPERIMENTAL SECTION

General Considerations. All manipulations were conducted using Schlenk techniques and at room temperature unless otherwise is stated. All solvents were rigorously dried prior to use. NMR spectra were recorded at 400.13 (^{1}H), and 100.62 (^{13}C) MHz on a Bruker AV400. Chemical shifts (δ) are given in ppm using $CDCl_3$ as solvent. ^{1}H and ^{13}C resonances were measured relative to solvent peaks considering TMS δ = 0 ppm. Elemental analyses were obtained on a Perkin-Elmer Series II 2400 CHNS/O analyser. Raman spectra were recorder in a Thermo Scientific DXR Raman Microscope. All reagents were commercially obtained and used without further purification. Compound $[Ru(CN^tBu)_4(Cl)_2]$ (**1**) was prepared as previously reported.[13]

General procedure for the reaction of $[Ru(CN^tBu)_4(Cl)_2]$ (1) and I_2. $\{[Ru(CN^tBu)_4(I)_2]\cdot I_2\}_n$ $(2\cdot I_2)_n$. In CH_2Cl_2: 0.075g (0.149 mmol) of $[Ru(CN^tBu)_4(Cl_2)]$ were dissolved in 20 ml of CH_2Cl_2, then 0.075 g (0.296 mmol) of I_2 were added. The solution acquired a dark brown colour. After 8 days stirring at room temperature 40 mL of hexane were added and the mixture was left standing until the diffusion of the solvents was complete. After 30 days compound $(\mathbf{2\cdot I_2})_n$ was isolated as black crystals. In EtOH: 0.030g (0.059 mmol) of $[Ru(CN^tBu)_4(Cl_2)]$, 0.030 g (0.118 mmol) of I_2, 25 ml of EtOH. After 8 days stirring, 50 ml of hexanes were added. After 8 days crystals of $(\mathbf{2\cdot I_2})_n$ were isolated. The reaction was performed in the dark and the result achieved was the same as in day light .^{1}H NMR ($CDCl_3$, 400MHz, 293K, δ ppm) 1.60 (s, 36H, ^{t}Bu). Elemental analysis: $RuC_{20}H_{36}N_4I_4$ cacld (%) C: 25.5 H: 3.9 N: 5.9. Found (%) C: 25.2 H: 4.0 N: 5.2

{[Ru(CN^{t}Bu)$_4$(Cl)$_2$]·2I$_2$}$_n$ (1·2I$_2$)$_n$: Following the described general procedure, the solution was stirred for 10 minutes , then 40 mL of hexanes were added and the mixture was left standing at 5ºC until the diffusion of the solvents was complete. After 5 days compound **(1•2I$_2$)$_n$** was isolated as red crystals. ^{1}H NMR ($CDCl_3$, 400MHz, 293K, δ ppm) 1.62 (s, 36H, ^{t}Bu). Elemental analysis: $C_{20}H_{36}Cl_2I_4N_4Ru$ cacld (%) C: 23.7 H: 3.5 N: 5.5. Found (%) C: 23.1 H: 3.4 N: 5.3

{[Ru(CN^{t}Bu)$_4$(Cl)(I)]·3I$_2$}$_n$ (3·3I$_2$)$_n$: Following the described general procedure, the reaction was stirred for one day and then one third of the solvent was removed under vacuum. The solution was left standing at 5ºC and after three days dark red crystals corresponding to **(3·3I$_2$)$_n$** were isolated. ^{1}H NMR ($CDCl_3$, 400MHz, 293K, δ ppm) 1.61 (s, 36H, ^{t}Bu). Elemental analysis: $C_{20}H_{36}ClI_7N_4Ru$ calcd (%) C: 17.7 H: 2.7 N: 4.1. Found (%) C: 18.1 H: 2.5 N: 3.9

Single-Crystal X-ray Structure Determinations of 1, (1·2I$_2$)$_n$, (2·I$_2$)$_n$, and (3·3I$_2$)$_n$. Details of the X-ray experiment, data reduction, and final structure refinement calculations are summarized in Table 2. Single crystals suitable for X-ray diffraction studies were selected for Data collection. The crystals were stuck to a glass fiber using an inert perfluorinated ether oil and mounted in a low temperature N_2 stream 200(2) K, in a Bruker-Nonius Kappa CCD single crystal diffractometer equipped with a graphite-monochromated Mo-Kα radiation (λ = 0.71073 Å), and an Oxford Cryostream 700 unit. The structures were solved by direct methods (SHELXS-97), using the WINGX package,[39] and completed by subsequent difference Fourier techniques and refined by using full-matrix least-squares against F^2 (SHELXL-97).[40] All non-hydrogen atoms were anisotropically refined. Most of the hydrogen atoms were geometrically placed and left riding on their parent atoms, and others were found in the Fourier difference maps. Absorption corrections for **1**, **(1·2I$_2$)$_n$, (2·I$_2$)$_n$,** and **(3·3I$_2$)$_n$** were performed with the programs SORTAV (semi-empirical from equivalent).[41] The crystal of **(3·3I$_2$)$_n$** was not of optimal quality and evident occupational disorder lowered the quality of the refinement. The disorder is

attributable to the presence of a small amount of the double substituted [$Ru(CNR)_4I_2$] complex, which could not be properly modeled. In fact the highest residual density (3.349 $Å^3$) appears near Cl1 (0.68 Å) and the biggest hole in the difference Fourier map of -3.336 $Å^3$ is located 0.48 Å from I6 (the iodine atom interacting with Cl1) which is in agreement with the presence of a small amount of the double substituted [$Ru(CNR)_4I_2$] complex in the crystal. As well, for **$(1\cdot 2I_2)_n$** a residual of electronic density of 3.895 $Å^3$ was found in the Fourier Difference map at 0.31 Å from Cl1, that can be assigned to the presence of small amounts of the monosubstituted complex [$Ru(CN^tBu)_4(Cl)(I)$].

Crystallographic data (excluding structure factors) for the structures reported in this paper have been deposited with the Cambridge Crystallographic Data Centre as supplementary publication no. CCDC-1039423 [**1**], CCDC-1039424 [**$(1\cdot 2I_2)_n$**], CCDC-1039425 [**$(2\cdot I_2)_n$**] and CCDC-1039426 [**$(3\cdot 3I_2)_n$**]. Copies of the data can be obtained free of charge on application to CCDC, 12 Union Road, Cambridge CB2 1EZ, UK (fax: (+44)1223-336-033; e-mail: deposit@ccdc.cam.ac.uk).

Table 2. Crystallographic Data for **1, $(1\cdot 2I_2)_n$, $(2\cdot I_2)_n$** and $(3\cdot 3I_2)_n$

Compound	**1**	$(1\cdot 2I_2)_n$	$(2\cdot I_2)_n$	$(3\cdot 3I_2)_n$
Formula	$C_{20}H_{36}Cl_2N_4Ru.C_7H_8$	$C_{20}H_{36}Cl_2I_4N_4Ru$	$C_{20}H_{36}I_4N_4Ru$	$C_{20}H_{36}ClI_7N_4Ru$
FW	596.63	1012.10	941.20	1357.35
Cryst size (mm^3)	0.37 x 0.31 x 0.25	0.44 x 0.34 x 0.15	0.35 x 0.30 x0.2	0.4 x 0.3 x 0.27
Color	Yellow	Red	Dark Red	Black
Cryst syst	Monoclinic	Tetragonal	Monoclinic	Orthorombic
Space group	$P2_1/c$	$P4_2/mnm$	$C2/c$	$Pnma$
a/ Å	16.869(2)	11.7096(11)	11.377(1)	22.735(3)
b/ Å	11.9137(8)	11.7096(11)	15.197(1)	14.945(2)
c/ Å	33.174(3)	13.7870(17)	18.484(3)	11.6353(12)
α (°)	90	90	90	90
β (°)	90.995(8)	90	106.64(2)	90
γ (°)	90	90	90	90
V/ $Å^3$	6665.9(12)	1890.4(3)	3062.0(6)	3953.4(8)
Z	8	2	4	4
ρ_{calcd}, g cm^{-3}	1.189	1.778	2.042	2.281
μ, mm^{-1}	0.650	3.835	4.558	5.945
F(000)	2496	948	1760	2464
θ range (deg)	3.01 to 27.50	3.48 to 27.54	3.53 to 27.64	3.21 to 25.31
θ comp. [%]	99.3	99.1	98.5	98.3
absorption correction	None	Multi scan	Multi scan	Multi scan
max. and min. transmission		0.19 0.222	0.755 1.405	0.042 0.083
Reflns collected	71802	31291	12189	18577
Indep reflns/ R(int)	15211/0.2373	1203/0.0766	3527/0.0767	3683/0.1114
Data/restraints/params	15211/24/613	1203/9/47	3527/0/402	3683/0/164
GOF	1.048	1.137	1.021	0.938
R_1, wR_2 [$I > 2\sigma(I)$] [a]	0.0806/0.1675	0.0645/ 0.1863	0.0440/0.0890	0.1302/0.3223
R_1, wR_2 [all data] [a]	0.1563/0.2120	0.0849/ 0.2134	0.0692/0.1011	0.1590/0.3422
Diff peak / hole (e $Å^{-3}$)	1.951/-1.547	3.895/-1.077	1.531/-1.610	3.349/-3.336

[a] $R_1 = \sum||F_0|-|F_c||/[\sum|F_0|]$; $wR_2 = \{[\sum w(F_0^2 - F_c)^2] / [\sum w(F_0^2)^2]\}^{1/2}$

Computational Details. All the calculations were performed at B97D-DFT[10] level of theory within the Gaussian 09 package.[42] The optimized model structures (distinguished by **m**) has methyl in place of *tert*-butyl substituents at the isonitrile ligands and their nature was corroborated by computed vibrational frequencies. All the optimizations were carried out with CPCM models[43] for either dichloromethane or methanol solvents. The effective Stuttgart/Dresden core potential (SDD)[11] was adopted for Ru and I atoms, while for all the other elements the basis set 6-31G was adopted including the polarization functions (d,p).

Qualitative MO arguments have been developed with the help of an EHMO analysis of the wave functions derived from CACAO package.[44]

ASSOCIATED CONTENTS

Supporting Information.

Electronic Supplementary Information available: Spectroscopic, structural data and computational details, including the picture of all the optimized structure nor reported in the main body of the paper and a list of all the optimized coordinates.

Corresponding Authors.

*E-mail: martaeg.mosquera@uah.es; pilar.gomez@uah.es; carlo.mealli@iccom.cnr.it

Notes

The authors declare no competing financial interest

ACKNOWLEDGEMENTS

We are grateful to the CREA Center and the project HP10 CHEVJ8 (CINECA) for computational resources. Financial support from Factoría de Cristalización-Consolider–Ingenio (CSD2006-00015) and the Alcalá University, Spain (CCG10-UAH/PPQ-5925) are gratefully acknowledged.

REFERENCES

1 (a) Desiraju, G. R.; Ho, P. S.; Kloo, L.; Legon, A. C.; Marquardt, R.; Metrangolo, P.; Politzer, P.; Resnati, G.; Rissanen, K. *Pure Appl. Chem.* **2013**, *85*, 1711-1713. (b) Metrangolo, P.;

Resnati, G. *Science* **2008**, *321*, 918-919 and ref. therein. (c) Gilday, L. C.; Robinson, S. W.; Barendt, T. A.; Lang, M. J.; Mullaney, B. R.; Beer, P. D. *Chem Rev.* **2015**, *115,* 7118-7195.

2. (a) Priimagi, A.; Cavallo, G.; Metrangolo, P.; Resnati, G. *Acc. Chem. Res.* **2013**, *46*, 2686-2695. (b) Fourmigue, M. *Struct Bond*, **2008**, *126*, 181-207

3. Voth, A. R.; Hays, F. A.; Ho, P. S. *Proc. Natl. Acad. Sci. USA* **2007,** *104*, 6188-6193.

4 Vidal, F.; Dávila, M. A.; San Torcuato, A.; Gómez-Sal, P.; Mosquera, M. E. G. *Dalton Trans*. **2013**, ***42***, 7074 -7084.

5 Manca, G.; Ienco, A.; Mealli, C. *Cryst. Growth & Design* **2012**, *12*, 1762-1771.

6 (a) Gunanathan, C.; Milstein, D. *Chem. Rev.*, **2014**, *114*, 12024–12087. (b) Giovanni, G. Di; Vaquer, L.; Sala, X.; Benet-Buchholz, J; Llobet, A. *Inorg. Chem.*, **2013**, *52*, 4335–4345. (c) Gutsulyak, D. V.; Vyboishchikov, S. F.; Nikonov, G. I. *J. Am. Chem. Soc.*, **2010**, *132*, 5950–5951.

7 (a) Zhou, Q.-X.; Lei, W.-H.; Sun, Y.; Chen, J.-R.; Li, C.; Hou, Y.-J.; Wang, X.-S.; Zhang, B.-W. *Inorg. Chem.*, **2010**, *49*, 4729-4731. (b) Howerton, B. S.; Heidary, D. K.; Glazer, E. C. *J. Am. Chem. Soc.*, **2012**, *134*, 8324–8327. (c) Clavel, C. M; Păunescu, E.; Nowak-Sliwinska, P.; Griffioen, A. W.; Scopelliti, R.; Dyson, P. J. *J. Med. Chem.*, **2015**, *58*, 3356–3365.

8 (a) Wang, M.; Gratzel, C.; Zakeeruddin, S. M.; Gratzel, M. *Energy Env. Sci.* **2012**, *5*, 9394-9405. (b) Baron, A; Herrero, C.; Quaranta, A.; Charlot, M.-F.; Leibl, W.; Vauzeilles, B.; Aukauloo, A. *Inorg. Chem.*, **2012**, *51*, 5985-5987 (c) Tuikka, M.; Hirva, P.; Rissanen, K.; Korppi-Tommolab, J.; Haukka, M. *Chem. Commun.* **2011**, *47*, 4499–4501.

9 (a) Nakatsuji, H; Sawamure, Y; Sakakura, A; Ishihara, K. *Angew. Chem. Int. Ed*, **2014**, *53*, 1-5. (b) Kniep, F.; Jungbauer, S. H.; Zhang, Q.; Walter, S. M.; Schindler, S.; Schnapperelle, I.; Herdtweck, E.; Huber, S. M. *Angew. Chem. Int. Ed*., **2013**, *52*, 7028–7032. (c) Manna, D.; Mugesh, G. *J. Am. Chem. Soc.*, **2012**, *134*, 4269–4279. (d) Beale, T. M.; Chudzinski, M. G.; Sarwar, M. G.; Taylor, M. S. *Chem. Soc. Rev.*, **2013**, *42*, 1667-1680. (e) Vapaavuori, J.;

Heikkinen, I. T. S.; Dichiarante, V.; Resnati, G.; Metrangolo, P.; Sabat, R. G.; Bazuin, C. G.; Priimagi, A.; Pellerin, C. *Macromolecules,* **2015**, *48*, 7535-7542.

10 Grimme, S. *J. Comp. Chem.* **2006**, *27*, 1787-1799.

11 Dolg, M; Stoll, H.; Preuss, H. ; Pitzer, R. M. *J. Phys. Chem.* **1993**, *97*, 5852-5859.

12 *e.g.* (a) Gray, L. R.; Gulliver, D. J.; Levason, W.; Webster, M. *Inorg. Chem.* **1983**, *22*, 2362-2366. (b) Le Bras, J.; Amouri, H.; Vaissermann, J. *Inorg. Chem.* **1998**, *37*, 924-926. (c) Andrews, M. B; Cahill, C. L. *Dalton Trans*., **2012**, *41*, 3911-3914. (d) Zordan, F.; Brammer, L.; Sherwood, P. *J. Am. Chem. Soc.*, **2005**, *127*, 5979–5989. (e) Johnson, M. T; Džolić, Z.; Cetina, M.; Wendt, O. F; Öhrström, L.; Rissanen, K. *Cryst. Growth Des.*, **2012**, *12*, 362–368.

13 Bassett, J. M.; Berry, D. E.; Barker, G. K.; Green, M.; Howard, J. A. K.; Stone, F. G. A. *J. Chem. Soc., Dalton Trans.* **1979**, 1003-1011.

14 *e.g.* Tuikka, M.; Niskanen, M.; Hirva, P.; Rissanen, K.; Valkonen, A.; Haukka, M. *Chem. Commun.* **2011**, *47*, 3427–3429.

15 *e.g.:* (a) Hitchcock, P. B.; Hughes, D. L.; Leigh, G.J.; Sanders, J. R.; de Souza, J.; McGarry, C. J.; Larkworthy, L. F. *J. Chem. Soc., Dalton Trans.* **1994**, 3683-3687. (b) Ilioudis, C. A.; Steed, J. W. *CrystEngComm* **2004**, *6*, 239-242. (c) Abate, A.; Brischetto, M.; Cavallo, G.; Lahtinen, M.; Metrangolo, P.; Pilati, T.; Radice, S.; Resnati, G.; Rissanen, K.; Terraneo, G. *Chem. Commun.* **2010**, *46*, 2724-2726.

16 Cambridge Structural Database System, Cambridge Crystallographic Data Centre, Cambridge, UK Version 5.32.

17 Yamamoto, Y.; Tanase, T.; Date, T.; Koide, Y.; Kabayashi, K. *Journal of Organomet. Chem.* **1990**, *386,* 365-374.

18 Parsons, R. *Handbook of Electrochemical Constants* **1959**, London Butterworths Scientific Publications. Reduction potentials are 2.87, 1.36, 1.09 and 0.53 V for the F, Cl, Br and I elements in the order.

19 Mitina, T. G.; Blatov, V. A. *Cryst. Growth & Design*. **2013***, 13,* 1655-1664.

20 Palmer, S. M.; Stanton, J. L.; Jaggi, N. K.; Hoffman, B. M.; Ibers, J. A.; Schwartz, L. H. *Inorg. Chem,* **1985**, *24*, 2040-2046.

21 Tebbe, K. -F.; Grafe-Kavoosian, A.; Freckmann, B. *Z. Naturforsch. B: Chem. Sci.* **1996**, *51*, 999.

22 Johnson, M. T.; Džolić, Z.; Cetina, M.; Wendt, O. F.; Öhrström, L.; Rissanen, K. *Cryst. Growth Des.* **2012**, *12*, 362−368.

23 Wurtemberger, M.; Ott, T.; Doring, C.; Schaub, T.; Radius U. *Eur. J. Inorg. Chem.* **2011**, 405-415.

24 (a) Herzberg, G. *"Infrared spectra of diatomic molecules*", 2ndnd edn. Van Nostrand, New Yersey, **1950**. (b) Brooks, W. V. F.; Crawford, B. J. *J. Chem. Phys.* **1954**, *23*, 363-365. (c) Klaboe, P. *J. Am. Chem. Soc.* **1967**, *89*, 3667-3676.

25 Wolters, L.P.; Bickelhaupt, F.M. *Chem. Open* **2012,** *1,* 96-105.

26 Deringer, V. L.; Englert, U.; Dronskowski, R. *Chem. Commun.* **2014**, *50*, 11547-11549.

27 Mulliken, R. S. *J. Am. Chem. Soc.* **1969**, *91*, 1237. (b) Mulliken, R. S. *Nobel Lecture December* **1966.**

28 (a) Wolters, L. P.; Schyman, P.; Pavan, M. J.; Jorgensen, W. L.; Bickelhaupt, F. M.; Kozuch, S. *WIREs Comput. Mol. Sci.* **2014**, *4*, 523-546. (b) Rosokha, S. V.; Stern, C. L.; Ritzert, J. T. *Chem. Eur. J.* **2013**, *19*, 8774-8788.

29 Rogachev, A. Y.; Hoffmann, R. *J. Am. Chem. Soc.* **2013**, *135*, 3262-3275.

30 (a) Pimentel, G.G. *J. Phys. Chem.,* **1951**, *19*, 446-448; (b) Rach, R. J.; Rundle, R. E. *J. Am. Chem. Soc.*, **1951**, *73*, 4321-4324.

31 Bigoli, F.; Deplano, P.; Ienco, A.; Mealli, C.; Mercuri, M. L.; Pellinghelli, M. A.; Pintus, G.; Saba, G.; Trogu, E. F. *Inorg. Chem.***1999**, *38*, 4626-4636.

32 Rossi, M.; Marzilli, L. G.; Kistenmacher, T. J. *Acta Crystallogr. Sect. B* **1978**, *34*, 2030-2033.

33 (a) Spackman, M. A.; Byrom, P. G. *Chem. Phys. Lett.* **1997**, *267*, 215-220. (b) McKinnon, J. J.; Mitchell, A. S.; Spackam, M. A. *Chem. Eur. J.* **1998**, *4*, 2136-2141.

34 (a) Saccone, M.; Cavallo, G.; Metrangolo, P.; Pace, A.; Pibiri, I.; Pilati, T.; Resnati, G.; Terraneo, G. *CrystEngComm* **2013**, *15*, 3102-3105. (b) Farina, A.; Meille, S. V.; Messina, M. T.; Metrangolo, P.; Resnati, G.; Vecchio, G. *Angew. Chem., Int. Ed.* **1999**, *38*, 2433-2436.

35 Schlosser, M. "*Organoalkali Chemistry*" Chapter (p. 61) of "Organometallics in Synthesis – Third Manual", John Wiley & Sons, Inc., Hoboken, New Jersey.

36 (a) Kumar, K.; Margerum, D. W. *Inorg. Chem.* **1987**, *26*, 2706-2711. (b) Kumar, K.; Day, A. R.; Margerum, D. W. *Inorg. Chem.***1986**, *25*, 4344-4350.

37 see for instance: R. A. Gossage, R. A.; Ryabov, A. D.; Spek, A. L.; Stufkens, D. J.; van Beek, J. A. M.; van Eldik, R.; van Koten, G. *J. Am. Chem. Soc.* **1999**, *121*, 2488-2497.

38 Rogachev, A. Y.; Hoffmann, R. *Inorg. Chem.* **2013**, *52*, 7161-7171.

39 Farrugia, L. J. *J. Appl. Cryst.* **1999**, *32*, 837-838.

40 Sheldrick, G. M. *Acta Cryst. A* **2008**, *64*, 112-122.

41 Blessing, R. H. *Acta Cryst A* **1995**, *51*, 33-38.

42 Gaussian 09, Revision D.01, Frisch, M. J.; Trucks, G. W.; Schlegel, H. B.; Scuseria, G. E.; Robb, M. A.; Cheeseman, J. R.; Scalmani, G.; Barone, V.; Mennucci, B.; Petersson, G. A.; Nakatsuji, H.; Caricato, M.; Li, X.; Hratchian, H. P.; Izmaylov, A. F.; Bloino, J.; Zheng, G.; Sonnenberg, J. L.; Hada, M.; Ehara, M.; Toyota, K.; Fukuda, R.; Hasegawa, J.; Ishida, M.; Nakajima, T.; Honda, Y.; Kitao, O.; Nakai, H.; Vreven, T.; Montgomery, J. A., Jr.; Peralta, J. E.; Ogliaro, F.; Bearpark, M.; Heyd, J. J.; Brothers, E.; Kudin, K. N.; Staroverov, V. N.; Kobayashi, R.; Normand, J.; Raghavachari, K.; Rendell, A.; Burant, J. C.; Iyengar, S. S.; Tomasi, J.; Cossi, M.; Rega, N.; Millam, J. M.; Klene, M.; Knox, J. E.; Cross, J. B.; Bakken, V.; Adamo, C.; Jaramillo, J.; Gomperts, R.; Stratmann, R. E.; Yazyev, O.; Austin, A. J.; Cammi, R.; Pomelli, C.; Ochterski, J. W.; Martin, R. L.; Morokuma, K.; Zakrzewski, V. G.; Voth, G. A.; Salvador, P.; Dannenberg, J. J.; Dapprich, S.; Daniels, A. D.; Farkas, Ö.; Foresman, J. B.; Ortiz, J. V.; Cioslowski, J.; Fox, D. J. Gaussian, Inc., Wallingford CT, **2009**.

43 (a) Barone, V.; Cossi, M. *J. Phys. Chem. A* **1998**, *102*, 1995-2001. (b) Cossi, M.; Rega, N.; Scalmani, G.; Barone, V. *J. Comput. Chem.* **2003**, *24*, 669-681.

44 (a) Mealli, C.; Proserpio, D. M. *J. Chem. Educ.* **1990**, *67*, 399. (b) Mealli, C.; Ienco, A.; Proserpio, D. M. Book of Abstracts of the XXXIII ICCC, Florence, Ed. CNR, Area della Ricerca di Firenze, **1998**, 510.

Table of Contents Graphic and Synopsis

Intriguing I_2 Reduction in the Iodide for Chloride Ligand Substitution at a Ru(II) Complex: Role of Mixed Trihalides in Redox Mechanisms.

M.E.G. Mosquera,* P. Gomez-Sal,* I. Diaz, L.M. Aguirre, A. Ienco, G. Manca, C. Mealli*

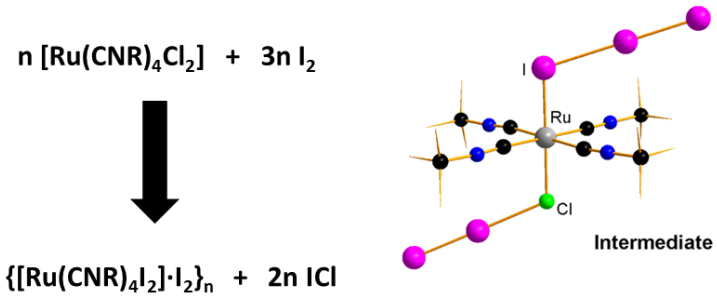

Reaction of $[Ru(CN^tBu)_4(Cl)_2]$ and I_2 affords the 1D species $\{[Ru(CN^tBu)_4I_2]\cdot I_2\}_n$ where the Cl^- have been substituted by I^- ligands. The result is intriguing in the absence of any suitable reducing agent for I_2. Reaction intermediates prompt the possible separation of ICl with a zerovalent Cl atom. The implied electron transfer over a trihalide foreshadows a dynamic behavior of halogen-bonding in solution, as corroborated by a theoretical analysis.